sciendo

PRODUCTION ENGINEERING ARCHIVES 2024, 30(2), 233-240

PRODUCTION ENGINEERING ARCHIVES

ISSN 2353-5156 (print)
ISSN 2353-7779 (online)

Exist since 4th quarter 2013
Available online at https://pea-journal.eu

Innovative acoustic emission method for monitoring the quality and integrity of ferritic steel gas pipelines

Grzegorz Świt[1*], Małgorzata Ulewicz[3], Robert Pała[2], Anna Adamczak-Bugno[1], Sebastian Lipiec[2], Aleksandra Krampikowska[1], Ihor Dzioba[2]

[1] Faculty of Civil Engineering and Architecture, Kielce University of Technology, Av. 1000-an. of Polish State 7, 25-314 Kielce, Poland; gswit@tu.kielce.pl (GŚ); aadamczak@tu.kielce.pl (AAB); akramp@tu.kielce.pl (AK)
[2] Faculty of Mechatronics and Mechanical Engineering, Kielce University of Technology, Av. 1000-an. of Polish State 7, 25-314 Kielce; rpala@tu.kielce.pl (RP); slipiec@tu.kielce.pl (SL); pkmid@tu.kielce.pl (ID)
[3] Faculty of Civil Engineering, Czestochowa University of Technology, 69 Dabrowskiego street, 42-201 Czestochowa; malgorzata.ulewicz@pcz.pl
*Correspondence: gswit@tu.kielce.pl

Article history
Received 10.01.2024
Accepted 03.04.2024
Available online 31.05.2024

Keywords
Pipelines,
Finite Element Method,
Stress,
Strain,
Acoustic Emission Method.

Abstract
This article presents a comprehensive improvement in the experimental analysis of cracking processes in smooth and sharp V-notched samples taken from gas transport pipelines, utilizing the acoustic emission (AE) method. The research aimed to establish a robust correlation between the failure mechanisms of uni-axially tensile samples and the distinct characteristics of AE signals for enhanced quality management in pipeline integrity. The study encompassed materials from two different straight pipe sections, encompassing both long-term used materials and new, unused materials. Through the application of the k-means grouping method to AE signal analysis, we achieved the identification of AE signal parameters characteristic of various stages of the material destruction process. This advancement introduces a significant improvement in monitoring and managing the operational safety of pipeline networks, offering a methodology that leverages advanced acoustic emission signal analysis. The outcomes present significant implications for the pipeline industry by proposing methods to enhance safety systems and more effectively manage the integrity and quality of gas infrastructure.

DOI: 10.30657/pea.2024.30.22

1. Introduction

As the demand for energy increases, the infrastructure for transporting fuels is expanding. The transmission systems used in most cases take the form of pipelines. Systems of this type are used, among others, for the transport of natural gas.

Gas pipelines enable the transportation of fuels over long distances within a given country or as part of international operations. These systems are generally considered to be one of the safest ways of transporting energy (Aljaroudi et al., 2015; Amyotte et al., 2016; Gumen et al., 2021, Kubicki, 2023). However, it is important to be aware that hazards such as material loss, pitting and cracks may occur in tubular conveying systems. Failures caused by the indicated factors and resulting from loads and environmental conditions may result in personal injury or death, economic losses and environmental damage (Alzyod and Ficzere, 2023; Benhamena et al., 2023; Bokůvka et al., 2018). Therefore, in the field of research, increasing attention is being paid to the inspection and monitoring of pipelines in order to conduct real-state maintenance of infrastructure and manage structural integrity.

In order to detect defects, it is important to constantly monitor the condition of gas pipelines. Over the last several decades, various external and internal monitoring methods have been proposed to detect pipeline leaks. They are known, among others: negative pressure wave (NPW) methods (Li et al., 2019), accelerometer-based techniques (Sun et al., 2016), acoustic emission (AE) technology (Jin et al., 2014), time domain reflectometry (Cataldo et al., 2012), distributed temperature sensing systems (F. Wang et al., 2017), ultrasonic technologies (Avelino et al., 2009), and magnetic flux leakage techniques (Feng et al., 2017). Among them, AE-based technologies have gained significant popularity due to their ability to quickly detect leaks, high sensitivity, real-time response, and ease of retrofitting (Hu et al., 2021; Liu et al., 2014).

A significant part of research related to the AE method uses primarily feature extraction and pattern recognition techniques regarding damage to build leak detection models. Xiao's team (Xiao et al., 2019) used wavelet features and support vector approach (SVM) to classify leaky and leaky states. Wang's research (L. Wang et al., 2017) extracted frequency width features from a time-domain signal pipeline and used them to train a support vector data description (SVDD) model for leak detection. Zadkarami (Zadkarami et al., 2017) used multi-layer perceptron neural network (MLPNN) and Dempster-Shafer classifier fusion technique to learn leakage patterns represented by statistical and wavelet-based features. Li (Li et al., 2017) suggested a leak detection approach based on kernel principal component analysis (KPCA) and SVM. Sun's team (Sun et al., 2016) used the envelope spectral entropy features obtained through local mean decomposition (LMD) of AE signals to train SVM and recognize leakage. Sun (Sun et al., 2016) further applied LMD and WT to extract RMS entropy features, which were then used to build an SVM leak detection model. In a study by Cui (Cui et al., 2016), empirical mode decomposition (EMD) was used to process non-stationary signals from pipelines and detect leaks in gas pipelines. Xu's team (Xu et al., 2013) used packet wavelet transform (WT) and time-domain features, such as mean value, peak value, RMS value, standard deviation, peak frequency, waveform index, and amplitude, in combination to identify leaks. with Fuzzy SVM.

The presented acoustic emission approaches are suitable for diagnosing leaks, but they pose problems in the assessment of real sections. The indicated supervised learning techniques require accurate data (signals) regarding pipeline failures. These approaches only detect advanced material destruction, which actually makes it impossible to take sufficiently early actions to limit media loss and prevent failure. According to the authors, a much better solution in the field of gas pipeline diagnostics is the use of signal databases containing signal classes corresponding to the processes occurring in the material, from elastic work to destruction (Świt et al., 2023, 2022). This action ensures the possibility of dynamic decision-making depending on the actual condition of the pipeline.

This article presents an experimental analysis of the cracking process of smooth and notched samples taken from pipes used for gas transport pipelines. The aim of these studies was to determine the characteristic parameters of AE signals corresponding to various stages of failure of uniaxially stretched, smooth and notched samples. The presented research is a stage in the development of a system for monitoring the metal condition of gas pipelines based on the analysis of acoustic emission signals.

2. Materials and testing methods

Samples for testing were taken from the pipes of the pipeline network for the transport of natural gas. For comparison, the material of two pipes was tested: S1 - pipe after long-term operation (40 years); and S4 – new pipe, not in use. It should be emphasized that these pipes were manufactured at a distant time and possibly in different steelworks, therefore no comparison of strength characteristics in terms of the reduction in time strength was carried out. In the steel of both pipes, there is a ferrite-pearlite microstructure with a grain size of 7 - 12 μm, however, for S4, thinner and more densely arranged plates were observed in the pearlite areas (Fig. 1a and 1b), which may be the result of faster cooling during the thermal treatment of the pipe. Extruded particles of MnS inclusions and single large spherical particles, probably of oxides, were also observed (Fig. 1c, 1d). The chemical composition of the steel of the tested pipes is shown in Table 1.

Table 1. Chemical composition of the steel of the tested pipes (according to the certificate)

Material	C [%]	Si [%]	S [%]	P [%]	Mn [%]	Al [%]
R35/G235/St37.0 - **S1**	0.17	0.35	0.040	0.04	0.35	0.02
L415NE - **S4**	0.23	0.45	0.015	0.025	1.4	0.06

Flat samples were made from straight pipe sections and then subjected to uniaxial loading. The tests were carried out according to PN-EN and ASTM (ASTM E8 / E8M-16ae1, 2016; PN-EN ISO 6892-1:2020-05, 2019) standards. The tests were carried out at a temperature of +20±2°C on a UTS/Zwick 100 testing machine, equipped with automated control and data recording systems. The samples were loaded to failure. During the test, signals of the force F and the elongation of the measuring part of the sample u_{ext} were recorded. An extensometer with a measurement base of 25 mm and a resolution of 0.001 mm was used to record the elongation of the sample.

Fig. 2 shows the nominal stress-strain diagrams ($\sigma - \varepsilon$). The values of basic strength and plasticity characteristics were determined on smooth samples. The obtained data indicate that S4 steel has higher values of strength characteristics σ_{YS} *i* σ_{UTS}. Also, the plasticity characteristics A_5 and Z are higher for material S4 (Table 2).

Table 2. Strength and plasticity characteristics of the tested steels

	$\sigma_{YS\_L}/\sigma_{YS\_H}$ [MPa]	σ_{UTS} [MPa]	E [GPa]	A [%]	Z [%]
S1	384/395	521	199	27	63
S4	413/420	585	205	38	76

Uniaxial tensile tests were also performed on sharply notched specimens. The introduction of a V-notch causes changes in the mechanical fields in the cross-section and leads to shear failure of the samples. A detailed analysis of mechanical fields in smooth and notched samples was presented in a previous work (Świt et al., 2023). The aim of these tests was to force the sample to fail according to the dominant shear mechanism and to record AE signals during loading and compare them with AE signals obtained on smooth samples (Fig. 3). Due to differences in the duration of tests of different samples, the results regarding the analysis of AE signals were presented in the normalized $t_n = t/t_{max}$. This format of presenting the results made it possible to compare the characteristics of AE signals on smooth and notched samples for the appropriate sections of sample deformation.

a)

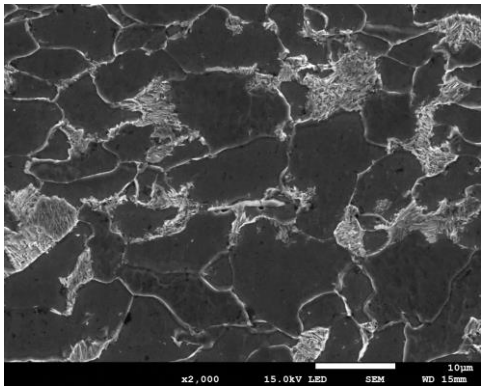

b)

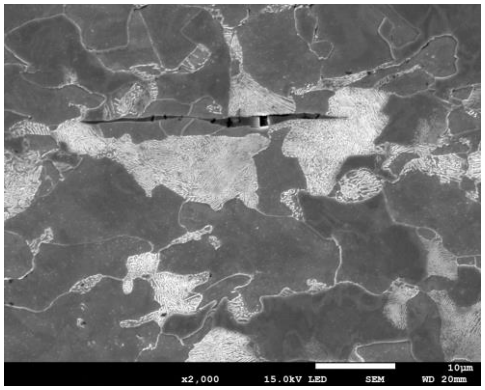

c)

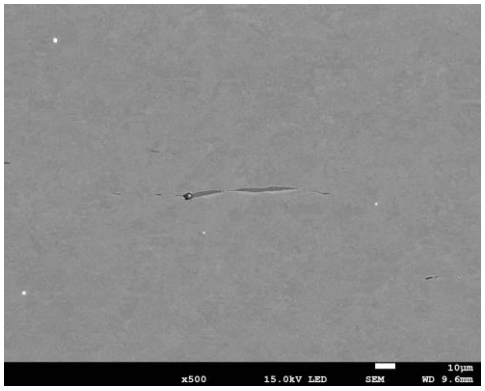

d)

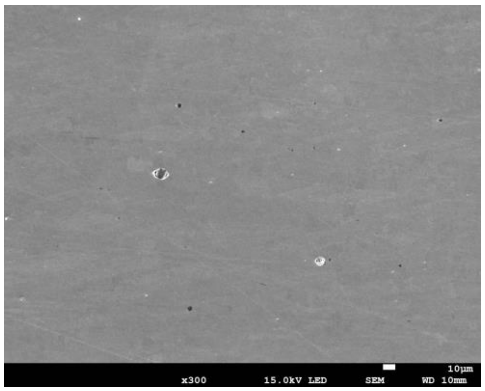

Fig. 1. Ferritic-perlitic microstructure of analysed steels: (a) – S1; (b) – S4, (x2000) and particles of non-metallic inclusions (c i d)

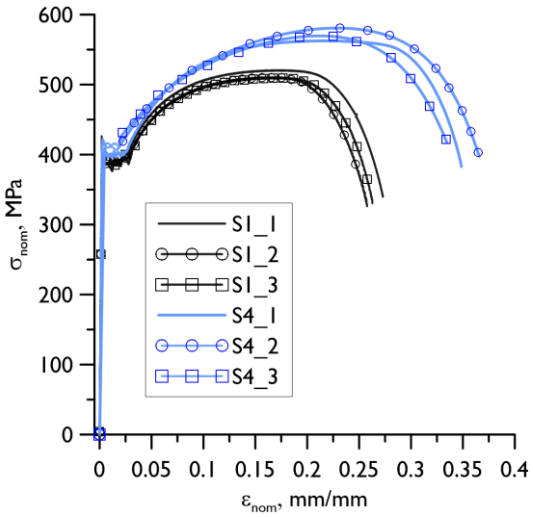

Fig. 2. The dependences of $\sigma - \varepsilon$ in nominal values for smooth specimens made of S1 (black) and S4 (blue) pipes

The recording and analysis of AE signals were performed using piezoelectric sensors and the Express-8 system (Mistras, Physical Acoustics). Sensors were used to record data in two measurement ranges:

- 1-20 kHz (VS12-E);
- 30-120 kHz (VS75-SIC-40dB)

The AE signals recorded during the tests were segregated and divided into 5 classes. For this purpose, the method presented in the works (Świt et al., 2023) was used.

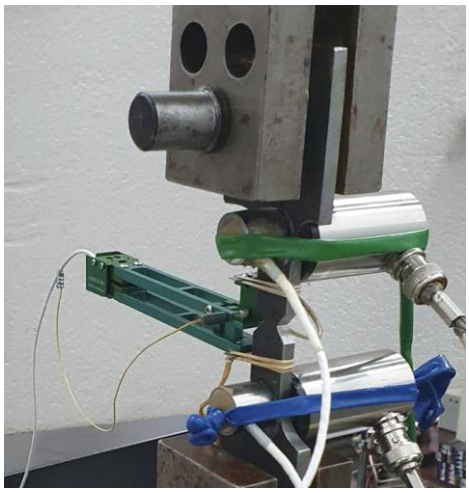

Fig. 3. Appearance of the tested specimen

3. Results and discussion

3.1. SEM testing of microstructure destruction

Metallographic tests were carried out on samples subjected to uniaxial stretching, the aim of which was to determine the characteristic mechanisms of destruction occurring in the microstructure at various stages of loading. The tests were performed on sections of smooth and V-notched samples taken

from pipes S1 and S4. This article presents the results for an S4 steel pipe. The results for S1 are similar and were partially presented in a previous publication (Świt et al., 2022).

During the strengthening of the material in the range of uniform deformation, up to the achievement of F_{max}, we do not observe any clear symptoms of destruction of the material's microstructure. Only a slight deformation of the ferrite grains, cracking of the extracted MnS particles and their decohesion (detachment) from the matrix can be observed (Fig. 4a, 4b).

a)

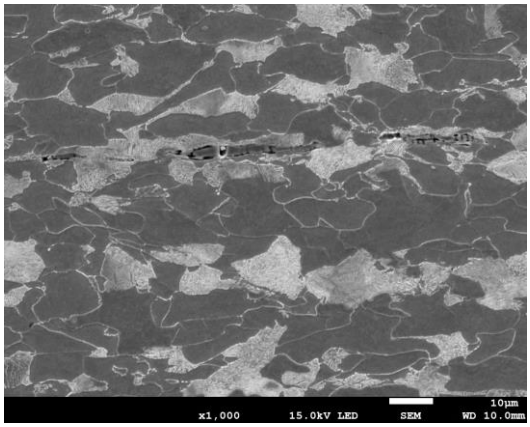

b)

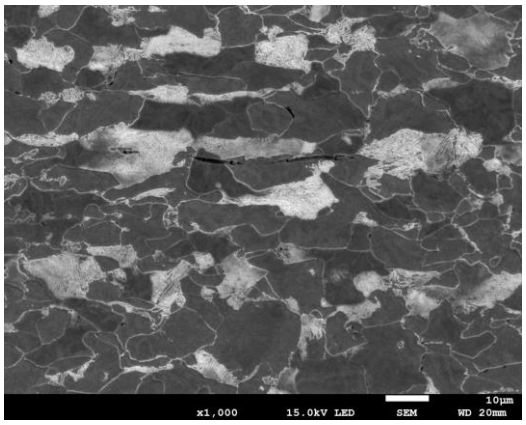

Fig. 4. Microstructure of samples in the range of uniform deformation just before neck formation: a) smooth, b) V-notched

In terms of neck formation, deformation of ferrite grains as well as cracking and decohesion from the matrix of inclusion particles were clearly observed in the material microstructure. In the neck material of smooth samples, these processes are more developed (advanced) (Fig. 5a, 5b).

Immediately before the destruction of the smooth sample material, we observe a large deformation of the ferrite grains (over 200%) and a developed destruction of the material between the ferrite and pearlite grains both in the direction parallel to the load and in the transverse direction (Fig. 6a). In the notched sample, the symptoms of material destruction are less visible, while the deformation of the ferrite grains is directed at an angle of ~30° (Fig. 6b).

a)

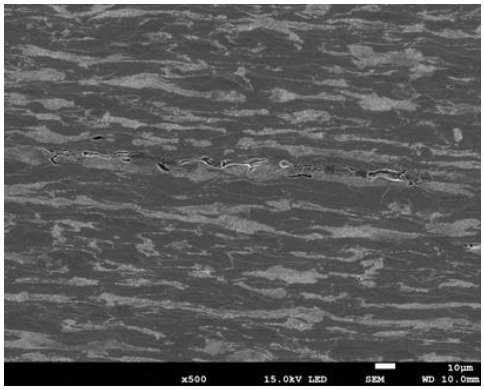

b)

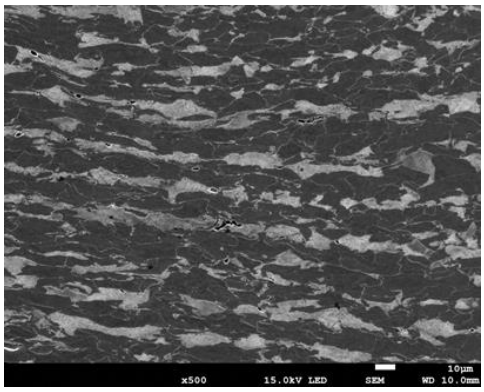

Fig. 5. Microstructure of samples in the range of neck formation: a) smooth, b) V-notched

a)

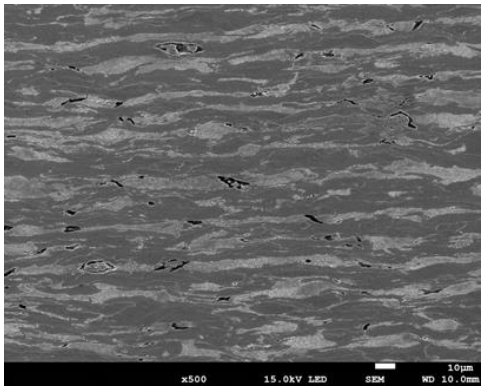

b)

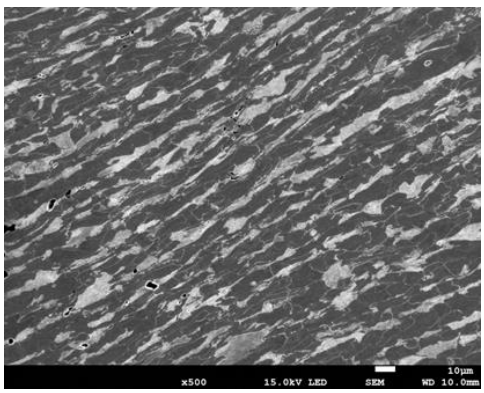

Fig. 6. Microstructure of samples immediately before destruction: a) smooth, b) V-notched

The development of plastic deformation at an angle is caused by a high level of shear stress in samples with sharp notches, which was analyzed in detail in a previous article (Świt et al., 2022), and leads to the failure of the sample according to the shear mechanism across the entire cross-section of the sample (Fig. 7b). Then, in the central part of the fracture of the smooth sample, there is an area where cracking developed due to the impact of the stress component normal to the cross-section, and only at the side surfaces - due to shear (Fig. 7a).

a)

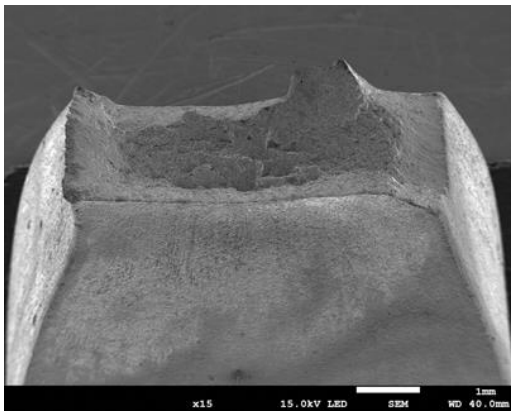

b)

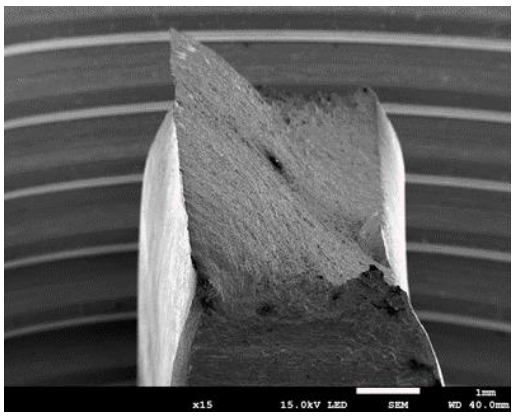

Fig. 7. The breakthroughs of the test specimens: a) smooth, b) V-notched

3.2. Acoustic Emissions (AE) signals analysis

Microstructure tests showed various symptoms of material destruction when loading samples - plastic deformation of grains, cracking of non-metallic inclusion particles, decohesion between particles and the matrix and between pearlite and ferrite phases, cracking of ferrite grains. These elementary acts of destruction emit AE signals with certain characteristic features. In order to determine these features in the AE signals recorded at various stages of the material destruction process while stretching the samples, a detailed analysis was carried out. As a result of the research, it was found that they sensitively respond to the type of destruction of quantities characterizing the energy (e.g. Energy, Signal Strength) and frequency (e.g. Average Frequency, Reverberation Frequency) of the signal and its shape (e.g. ASL, RMS). Due to the fact that the loading durability of the tested samples was different, the time was also given in normalized form: $t_{norm} = t/t_{max}$.

Based on previous experience (Świt et al., 2022), the analysis took into account AE signals recorded in various ranges of deformation of samples with amplitude levels > 40 dB and with high values of energy characteristics (Energy or Signal Strength). AE signals were grouped according to a non-hierarchical approach (*k-means* algorithm) (Świt et al., 2023, 2022).

Against the background of stress-time graphs in normalized values, the courses of appropriate characteristics of AE signals for samples made of pipe material S1 and S4 are presented (Fig. 8-10). Fig. 8 shows changes in the Average Frequency value during loading samples. Despite large data scatters, it can be seen that the minimum values of the Average Frequency occur when the samples are completely destroyed. For smooth and notched samples made of pipe S4, compared to S1, lower values were observed in terms of uniform elongation and higher values at the moment of failure.

The ASL level reaches its highest values when the samples are destroyed. In S4 steel samples, the ASL level, initially lower than S1 in terms of uniform elongation, exceeds the values of S1 samples at the moment of complete failure (Fig. 9).

a)

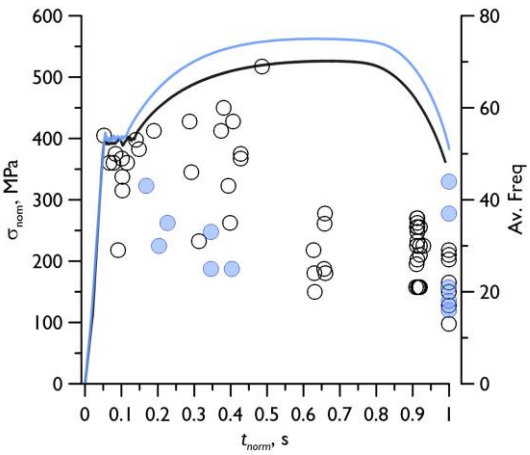

b)

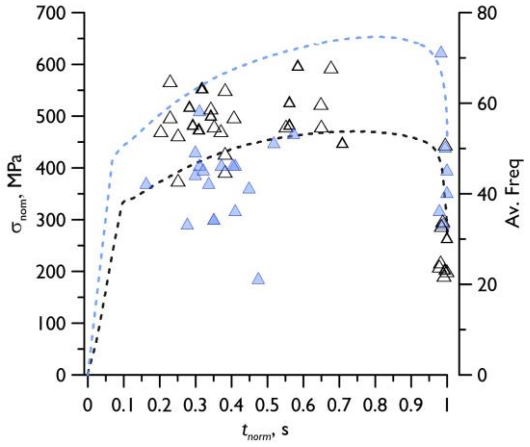

Fig. 8. Distribution of the Average Frequency parameter over time: (a) for smooth samples S1 and S4; (b) for notched samples S1 and S4 (b) [S1 - empty symbols; S4 – filled symbols]

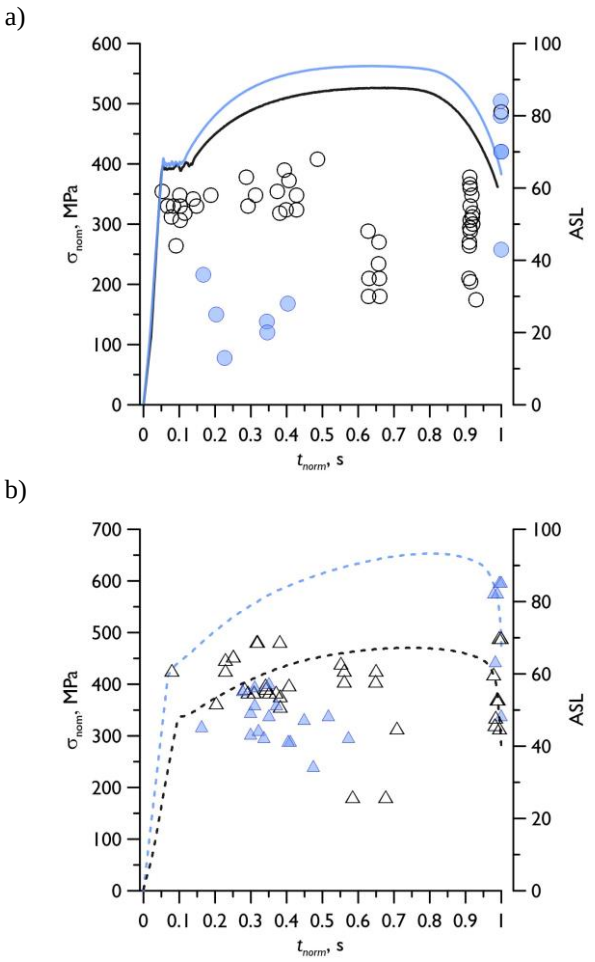

Fig. 9. Distribution of the ASL parameter over time: (a) for smooth samples S1 and S4; (b) for notched samples S1 and S4 [S1 - empty symbols; S4 – filled symbols]

Figures 10 show the distributions of Signal Sterngth characteristics during loading of smooth and notched samples. The figures show signals segregated into classes in accordance with the assumptions described in studies (Świt et al., 2022). AE signals with very high Signal Strength values (>4.3E07 pv·s) and a dark blue color (class 1) usually occur when the sample is completely destroyed. Occasionally, high levels of Signal Strength characteristics were also observed in other intervals - during uniform sample deformation or just before neck formation (Fig. 10). Based on the observation of microstructure sections (Fig. 4), it can be concluded that in the section of uniform deformation, these signals are most likely emitted as a result of the cracking of non-metallic inclusion particles. Therefore, class 1 signals occur during the cracking of microstructure components - non-metallic inclusion particles, pearlite plates and ferrite grains. These signals are characterized by relatively low frequency values - Average Frequency in the range of 15-35 kHz, and relatively high values of the ASL parameter - 70-85. It should be noted that the maximum Signal Strength values recorded at the moment of complete destruction of samples from pipe S4 are higher compared to S1

The next group of signals marked as class 3 (blue) occurs in the entire range of plastic deformations. The Signal Strength values for these signals are in the interval $7.5E^{06}$-$8.5E^{07}$ pv·s, Average Frequency range 17-60 kHz and ASL 20-65. In samples from the S4 pipe, the frequency and ASL values are usually lower than in the S1 samples. Taking into account metallographic tests, it can be concluded that these signals arise during plastic deformation of the material and the decohesion process between ferrite and particles of non-metallic inclusions and between particles of pearlite and ferrite phases.

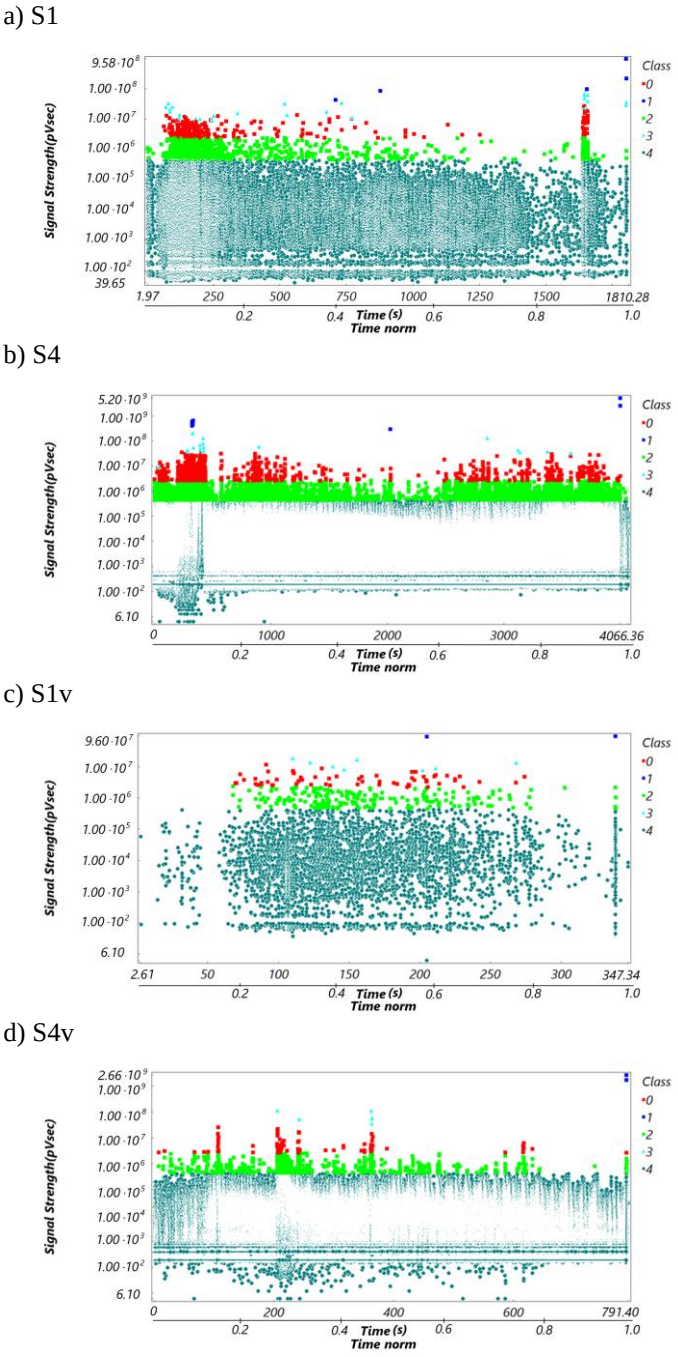

Fig. 10. Distribution of the Signal Strength parameter over time for samples from pipes S1 and S4: (a and b) for smooth; (c, d) for V-notch samples

Signals from classes 0 (red) and 2 (light green) occur in the range of plastic deformation of the material. These signals have similar frequency ranges and differ in Signal Strength. It can therefore be assumed that they are generated by plastic deformations of the material of varying intensity.

The most numerous group of signals (class 4) with a low Signal Strength level (< 4.4E05 pv·s) emitted by various other factors of the load process and can be treated as "technological noise".

4. Summary and conclusions

Based on the above-presented research results on the cracking process of ferritic-pearlite steel from pipes S1 and S4, certain generalizations were formulated.

When loading uniaxially smooth and V-notched tensile samples, various mechanisms of material destruction occur: plastic deformation of the matrix (mainly ferrite grains), decohesion between inclusion particles and the ferritic matrix of the material, cracking of MnS inclusion particles and coagulated particles of precipitates at the grain boundaries, cracking of ferrite grains.

Plastic deformation is present at every stage of the material destruction process when samples are stretched. The dominant stage of this process is the uniform deformation of the sample material until a neck is formed. The range of Average Frequency values in this interval is in the band 20-70 kHz. However, for samples from pipe S4 it is lower than for S1 (Fig. 8). The process of plastic deformation at this stage is also accompanied by decohesion and local cracks in the pearlitic phase of the material. At the moment of fracture of smooth and notched samples S1 and S4, signals with the highest Signal Strength levels occur. The appropriate frequency for these signals is in the range of 15-30 kHz and high ASL values (70-85).

Comparing the AE signals of smooth and V-notched samples, it can be seen that the notched samples have a lower level of Signal Strength. Also in them, a smaller number of class 3 signals was observed, which may indicate that the decohesion process in the material of these samples is less advanced. This was caused by differences in the stress state in smooth and V-notched samples (Świt et al., 2023).

Comparing the materials of S1 and S4 pipes, it was found that S4 has higher strength and plasticity characteristics (Table 2). The characteristic values for AE signals are also slightly different for S1 and S4 materials. The Signal Strength values for the signals recorded at the moment of fracture for S4 are higher than for S1 for the appropriate types of samples, smooth (Figs: 10a, 10b) and V-notch (Figs. 10c, 10d). So this indicates that there is a correlation between the material strength characteristics and the AE signal power.

During tests of smooth and notched samples from pipes S1 and S4, AE signals with qualitatively similar characteristics were recorded. In samples made of S4 steel, compared to S1, a smaller number of AE signals from classes 3, 0, 1 were recorded. This may be due to the better quality of S4 steel, made nowadays according to modern technology. During metallographic tests, a smaller number of extracted MnS particles was noticed in the steel from the S4 pipe compared to S1.

The presence of signals of classes 2 and 0 indicates the development of plastic deformations in the material.

The occurrence of class 3 signals means that the material is cracking non-metallic inclusion particles and decohesing between these particles and the ferritic matrix.

Registration of class 1 signals indicates that a crack development process is taking place in the material - micro cracks are merging and/or the crack is propagating.

The presented test results provide the basis for the conclusion that the acoustic emission method can be very useful for assessing the technical condition of gas pipelines made of steel material. Thanks to the use of this technique, it is possible to determine the processes occurring in the material and to correlate acoustic signals with the mechanical parameters of steel. Improving monitoring and measurement processes by units managing gas infrastructure and external entities is currently the basic solution to maintain the quality and security of gas supplies.

Reference

Aljaroudi, A., Khan, F., Akinturk, A., Haddara, M., Thodi, P., 2015. Risk assessment of offshore crude oil pipeline failure. Journal of Loss Prevention in the Process Industries, 37, 101–109. DOI: 10.1016/j.jlp.2015.07.004

Alzyod, H., Ficzere, P., 2023. Correlation Between Printing Parameters and Residual Stress in Additive Manufacturing: A Numerical Simulation Approach. Production Engineering Archives, 29, 279–287.

Amyotte, P.R., Berger, S., Edwards, D.W., Gupta, J.P., Hendershot, D.C., Khan, F.I., Mannan, M.S., Willey, R.J., 2016. Why major accidents are still occurring. Current Opinion in Chemical Engineering. Biotechnology and bioprocess engineering / Process systems engineering, 14, 1–8. DOI: 10.1016/j.coche.2016.07.003

ASTM E8 / E8M-16ae1, 2016. ASTM E8 / E8M-16ae1, Standard Test Methods for Tension Testing of Metallic Materials. ASTM International, West Conshohocken.

Avelino, Á.M., de Paiva, J.Á., da Silva, R.E.F., de Araujo, G.J.M., de Azevedo, F.M., de O. Quintaes, F., Maitelli, A.L., Neto, A.D.D., Salazar, A.O., 2009. Real time leak detection system applied to oil pipelines using sonic technology and neural networks, in: 2009 35th Annual Conference of IEEE Industrial Electronics. Presented at the 2009 35th Annual Conference of IEEE Industrial Electronics, pp. 2109–2114. DOI: 10.1109/IECON.2009.5415324

Benhamena, A., Fatima, B., Foudil, K., Baltach, A., Chaouch, M.I., 2023. Numerical Analysis of Fracture Behavior of Functionally Graded Materials using 3D-XFEM. Advances in Materials Science, 23, 33–46.

Bokůvka, O., Jambor, M., Trško, L., Nový, F., Lisiecka, B., 2018. Fatigue lifetime of 20MnV6 steel with holes manufactured by various methods. Production Engineering Archives, 19, 3–5. DOI: 10.30657/pea. 2018.19.01

Cataldo, A., Cannazza, G., De Benedetto, E., Giaquinto, N., 2012. A New Method for Detecting Leaks in Underground Water Pipelines. IEEE Sensors Journal, 12, 1660–1667. DOI: 10.1109/JSEN.2011.2176484

Cui, X., Yan, Y., Ma, Y., Ma, L., Han, X., 2016. Localization of CO2 leakage from transportation pipelines through low frequency acoustic emission detection. Sensors and Actuators A: Physical, 237, 107–118. DOI: 10.1016/j.sna. 2015.11.029

Kubicki, K., 2023. Technical and economic aspects of load-bearing welded joints in reinforcing steel. Construction of Optimized Energy Potential, 12(1), 228–235. DOI: 10.17512/bozpe.2023.12.25

Feng, J., Li, F., Lu, S., Liu, J., Ma, D., 2017. Injurious or Noninjurious Defect Identification From MFL Images in Pipeline Inspection Using Convolutional Neural Network. IEEE Transactions on Instrumentation and Measurement, 66, 1883–1892. DOI: 10.1109/TIM.2017.2673024

Gumen, O., Ujma, A., Kruzhkova, M., 2021. Research into the process of spraying complex titanium and zirconium nitride on structural steel and reaction times relating to the final finish and quality obtained. Construction of Optimized Energy Potential, 10, 71–76. DOI: 10.17512/bozpe.2021.1.07

Hu, Z., Tariq, S., Zayed, T., 2021. A comprehensive review of acoustic based leak localization method in pressurized pipelines. Mechanical Systems and Signal Processing, 161, 107994. DOI: 10.1016/j.ymssp.2021.107994

Jin, H., Zhang, L., Liang, W., Ding, Q., 2014. Integrated leakage detection and localization model for gas pipelines based on the acoustic wave method. Journal of Loss Prevention in the Process Industries, 27, 74–88. DOI: 10.1016/j.jlp.2013.11.006

Li, J., Zheng, Q., Qian, Z., Yang, X., 2019. A novel location algorithm for pipeline leakage based on the attenuation of negative pressure wave. Process Safety and Environmental Protection, 123, 309–316. DOI: 10.1016/j.psep. 2019.01.010

Li, Z., Zhang, H., Tan, D., Chen, X., Lei, H., 2017. A novel acoustic emission detection module for leakage recognition in a gas pipeline valve. Process Safety and Environmental Protection, 105, 32–40. DOI: 10.1016/j.psep. 2016.10.005

Liu, C., Li, Y., Meng, L., Wang, W., Zhang, F., 2014. Study on leak-acoustics generation mechanism for natural gas pipelines. Journal of Loss Prevention in the Process Industries, 32, 174–181. DOI: 10.1016/j.jlp. 2014.08.010

PN-EN ISO 6892-1:2020-05, 2019. PN-EN ISO 6892-1:2020-05, Metallic materials — Tensile testing — Part 1: Method of test at room temperature. International Organization for Standardization, Geneva.

Sun, J., Xiao, Q., Wen, J., Zhang, Y., 2016. Natural gas pipeline leak aperture identification and location based on local mean decomposition analysis. Measurement, 79, 147–157. DOI: 10.1016/j.measurement.2015.10.015

Świt, G., Dzioba, I., Adamczak-Bugno, A., Krampikowska, A., 2022. Identification of the Fracture Process in Gas Pipeline Steel Based on the Analysis of AE Signals. Materials, 15, 2659. DOI: 10.3390/ma15072659

Świt, G., Dzioba, I., Ulewicz, M., Lipiec, S., Adamczak-Bugno, A., Krampikowska, A., 2023. Experimental-numerical analysis of the fracture process in smooth and notched V specimens. Production Engineering Archives, 29, 444–451. DOI: 10.30657/pea.2023.29.49

Wang, F., Lin, W., Liu, Z., Wu, S., Qiu, X., 2017. Pipeline Leak Detection by Using Time-Domain Statistical Features. IEEE Sensors Journal, 17, 6431–6442. DOI: 10.1109/JSEN.2017.2740220

Wang, L., Narasimman, S.C., Reddy Ravula, S., Ukil, A., 2017. Water Ingress Detection in Low-Pressure Gas Pipelines Using Distributed Temperature Sensing System. IEEE Sensors Journal, 17, 3165–3173. DOI: 10.1109/JSEN.2017.2686982

Xiao, R., Hu, Q., Li, J., 2019. Leak detection of gas pipelines using acoustic signals based on wavelet transform and Support Vector Machine. Measurement, 146, 479–489. DOI: 10.1016/j.measurement.2019.06.050

Xu, Q., Zhang, L., Liang, W., 2013. Acoustic detection technology for gas pipeline leakage. Process Safety and Environmental Protection, 91, 253–261. DOI: 10.1016/j.psep.2012.05.012

Zadkarami, M., Shahbazian, M., Salahshoor, K., 2017. Pipeline leak diagnosis based on wavelet and statistical features using Dempster–Shafer classifier fusion technique. Process Safety and Environmental Protection, 105, 156–163. DOI: 10.1016/j.psep.2016.11.002